THE NATURE OF THE CONTINENTAL CRUST, HARDEMAN COUNTY, TEXAS, U.S., AS SEEN ON WAVE EQUATION MIGRATED DEEP SEISMIC REFLECTION SURVEYS

Heloise Bloxsom

Introduction

Geophysicists have traditionally been interested in the nature of the crust and the crust-mantle interface. Our knowledge of the deep continental crust has been inferred chiefly from gravity, magnetics, seismic refraction, and electro-magnetic methods. Recently COCORP (Consortium for Continental Reflection Profiling) has been gathering 12 and 24 fold VIBROSEIS[1] seismic reflection data to learn more about the crust and upper mantle. This represents the highest multiplicity to date in deep crustal seismic reflection work. However, all previous articles (Oliver et al., 1976; Oliver and Kaufman, 1977) have interpreted unmigrated sections, wherein significant diffractions and the incorrect spatial location of dipping energy hindered accurate interpretation. This paper presents an interpretation of 3 migrated profiles in Hardeman County, Texas, the first study area of COCORP. Figure 1 shows the location of these lines. Petty-Ray Geophysical shot and processed this data. Field procedures are described in the appendix to this paper.

There were three outstanding incentives to migrate these deep crustal sections. First, we do see deep reflections on the unmigrated data. Secondly, we know from a nearby well that basement (Precambrian rhyolite, age 1265 $\pm$ 40 m.y.) starts at 1.6 sec (~3 km)

[1] registered trademark of Continental Oil Co.

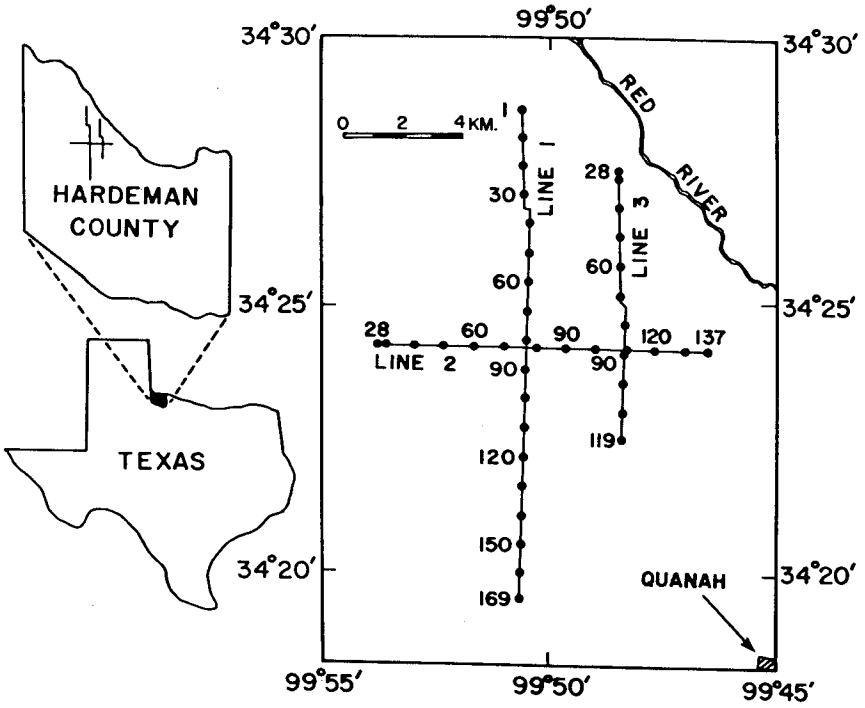

FIGURE 1. -- Location map for seismic profiles in Hardeman County, Texas. Selected station numbers are indicated (from Oliver et al., 1976).

(Oliver et al., 1976). The rest of the seismic section with nearly constant interval velocities of ~5.5 - 6.5 km/sec to about 11 sec is thought to consist of the igneous and metamorphic rocks known to be older than the rhyolite. Thirdly, we find very good penetration of relative high frequencies deep within the basement. Assuming a Q of 100 for the crust, frequencies on the order of 10 hz or less are expected at 10 sec.

$$100 > (\text{two way travel time}) \times \text{freq.}$$

However, we see some 25 hz signal at 10 sec. which indicates that (1) a Q of 100 may be too low for this area, and (2) due to the presence of higher frequencies, better resolution than normally encountered is present here.

Method

At Stanford a frequency domain (constant velocity) migration algorithm is available to migrate large data sets in quite reasonable execution times. On our minicomputer, a large data set would be 168 to 325 traces - 1875 time points. The necessary padding with zeroes yields a 1024 trace - 4096 time sample matrix to be migrated. With a nearly constant velocity section below 1.6 sec., using a constant velocity migration algorithm is justifiable. The data were migrated first with a velocity of 6 km/sec to image the deeper crust, and then remigrated at 5 km/sec to delineate faulting in the upper horizons (3 - 4 sec). The migration of these data sets is described by Ottolini (SEP 14); the algorithm is described by Stolt (1978) and Lynn (SEP 11).

Observations

The primary effect of migration was to enhance dip continuity and thus emphasize the layered heterogeneous nature of the crust at this location. Figure 2 shows portions from the unmigrated and migrated versions of line 2. Figure 3 shows the entire unmigrated and migrated versions of line 1. Layering in specific depth intervals within certain lateral limits, is observed. Several of the layered zones are recognizable on 2 to 3 profiles. An outline map of these horizons is shown on Figure 4.

Figure 2. (next two pages) The unmigrated (left) and migrated (right) versions of line 2. Migrated at 6 km/sec to image between ~6 to ~11 sec. East is to the right; the line is ~11 km long. Scale is 1:1.

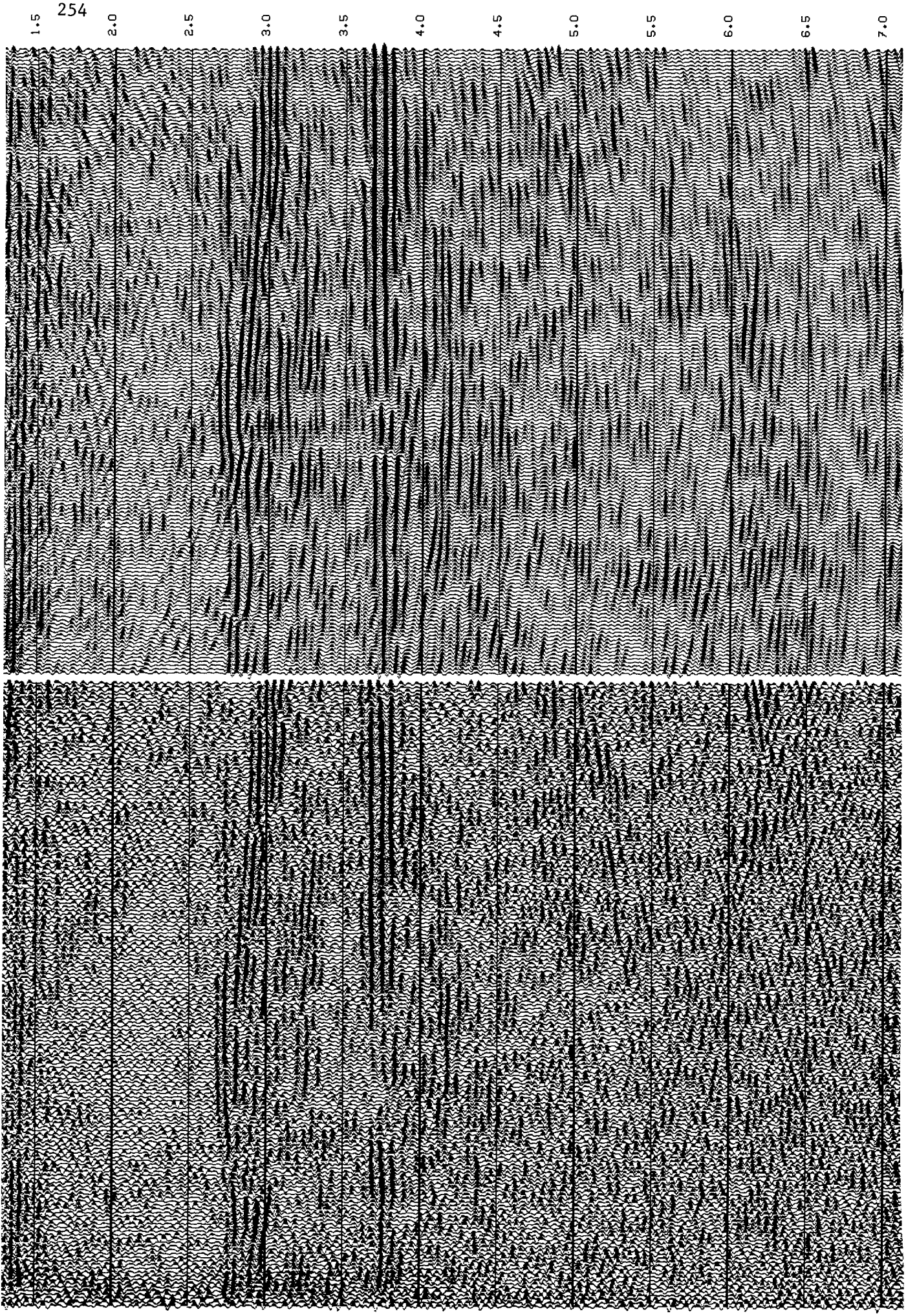
1.5
2.0
2.5
3.0
3.5
4.0
4.5
5.0
5.5
6.0
6.5
7.0

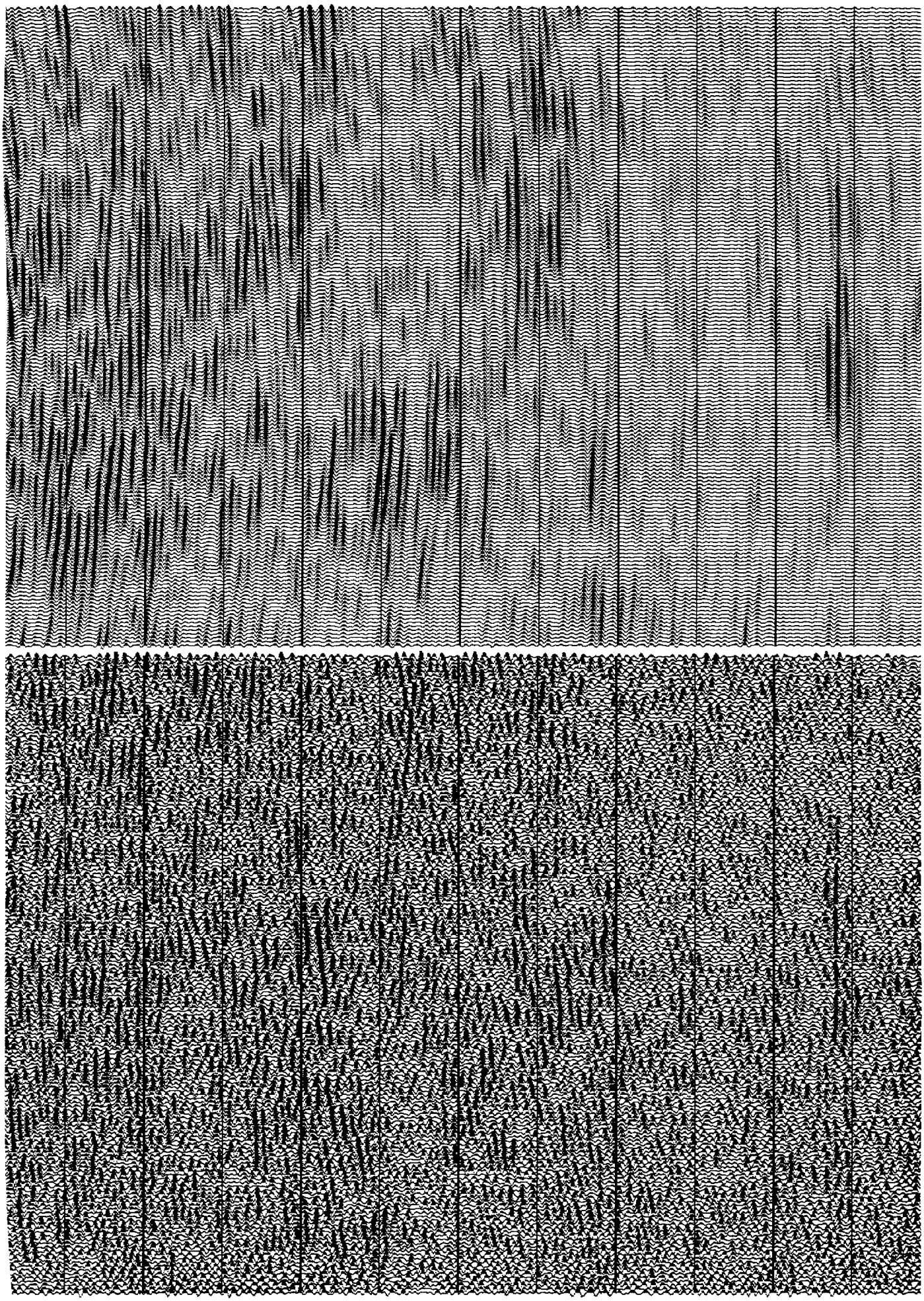
7.5
8.0
8.5
9.0
9.5
10.0
10.5
11.0
11.5
12.0
12.5

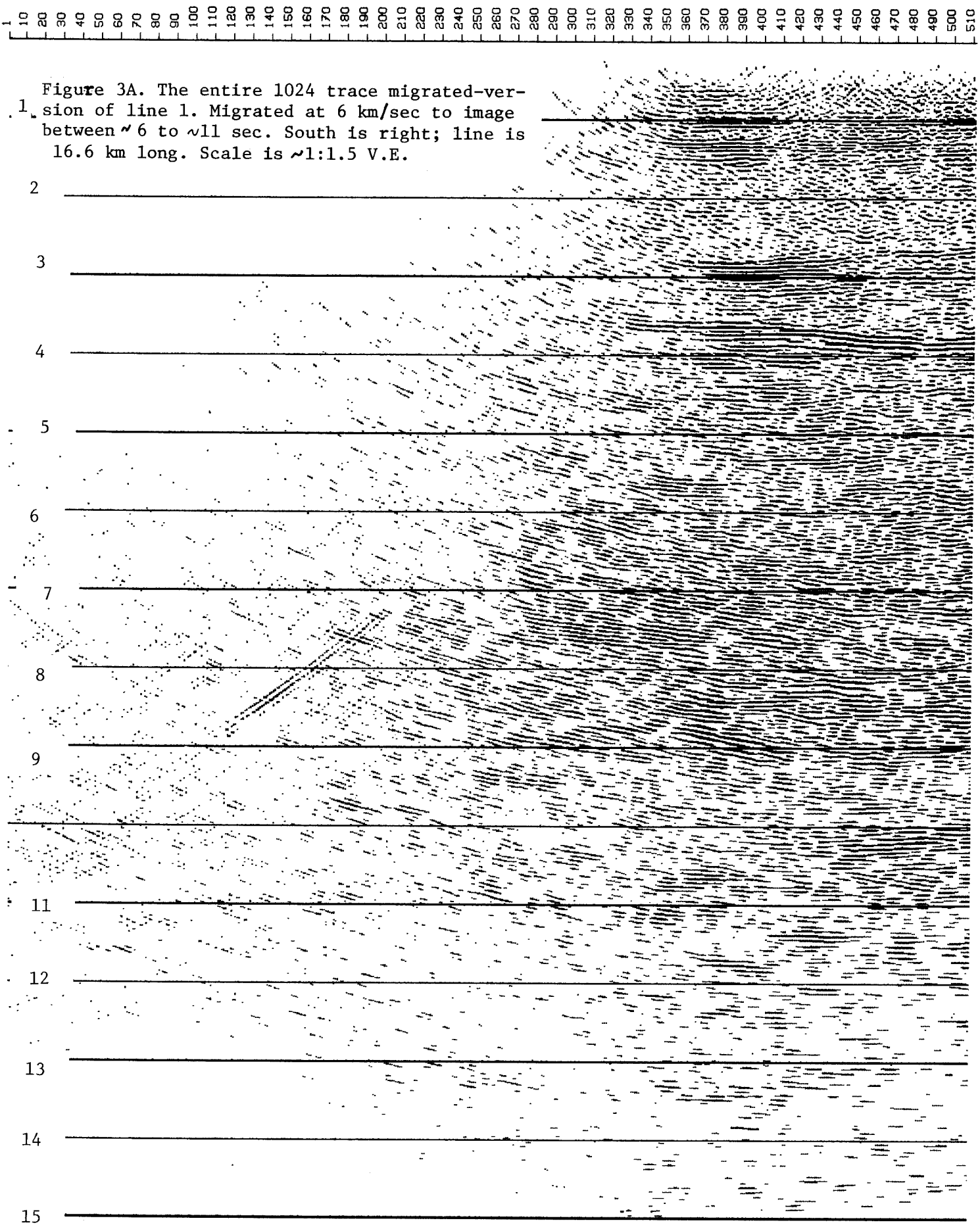

Figure 3A. The entire 1024 trace migrated-version of line 1. Migrated at 6 km/sec to image between ~6 to ~11 sec. South is right; line is 16.6 km long. Scale is ~1:1.5 V.E.

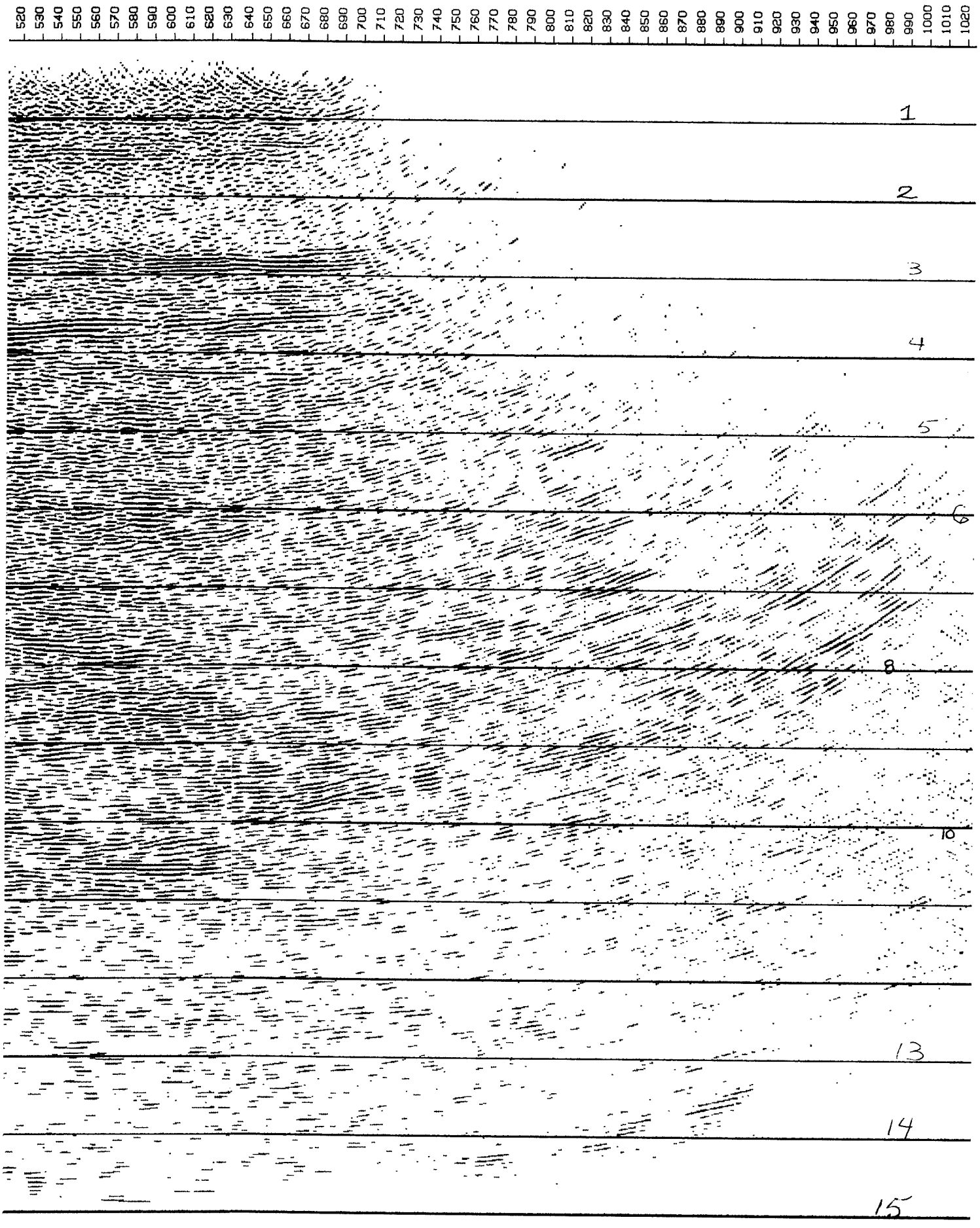
520 530 540 550 560 570 580 590 600 610 620 630 640 650 660 670 680 690 700 710 720 730 740 750 760 770 780 790 800 810 820 830 840 850 860 870 880 890 900 910 920 930 940 950 960 970 980 990 1000 1010 1020
1
2
3
4
5
6
8
10
13
14
15

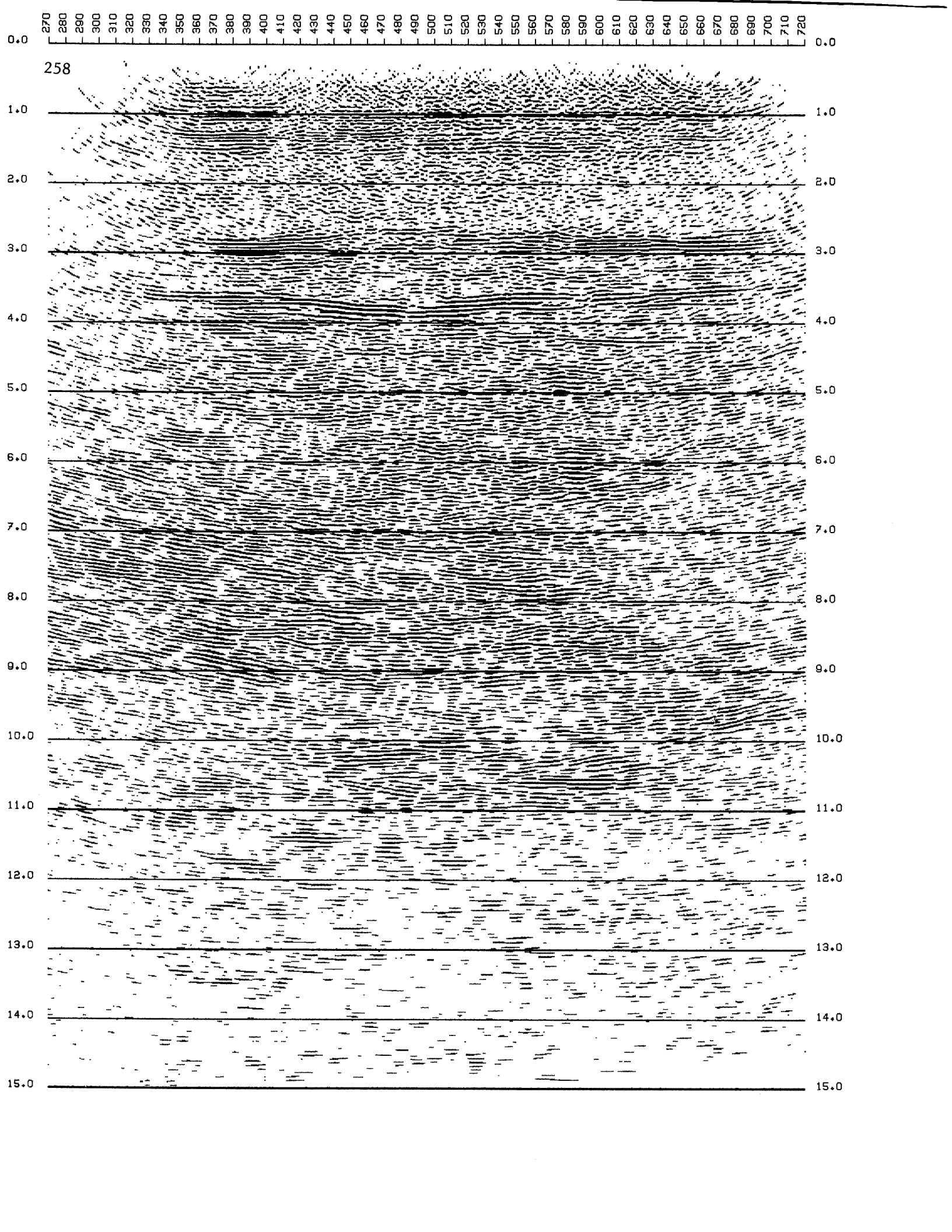
270 280 290 300 310 320 330 340 350 360 370 380 390 400 410 420 430 440 450 460 470 480 490 500 510 520 530 540 550 560 570 580 590 600 610 620 630 640 650 660 670 680 690 700 710 720
0.0
258
1.0
2.0
3.0
4.0
5.0
6.0
7.0
8.0
9.0
10.0
11.0
12.0
13.0
14.0
15.0

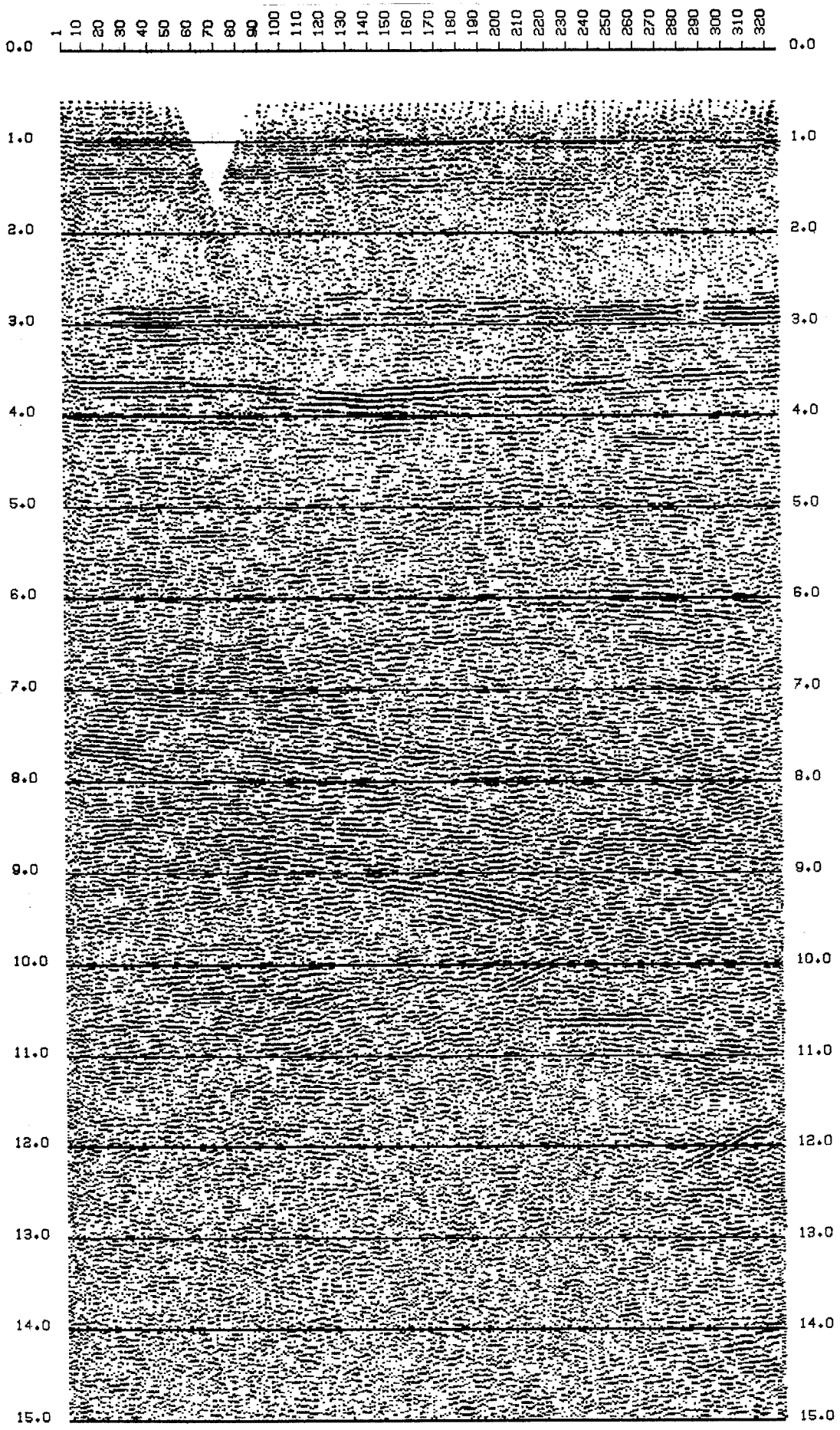

Figure 3B. (left and right) The center portion of figure 3A (migrated line **1)** is reproduced on the left (to avoid the binding's crease). On the right is the unmigrated line 1. Migration was at 6 km/sec to image between ~6 to ~11 sec. South is to the right; numbers on the top are the trace numbers, not shotpoint (station) numbers. 1:1.5 V.E.

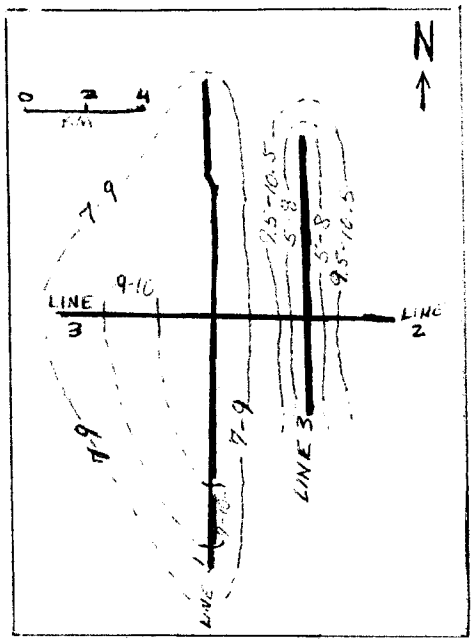

FIGURE 4 -- Outlines showing extent of five layered dense-reflector zones. (Numbers are in seconds.)

Faulting in the upper horizons above 4 sec is suggested on the unmigrated sections. As expected, migration delineated the faults. (See. Fig. 5, migrated line 2, 5 km/sec, v.e. 1:2).

We see an abrupt termination of layered reflectors below 11 sec. on lines 1 and 2. Oliver et al. also reported this discontinuity in their interpretation of the unmigrated data. Laminated reflectors between 10 and 11 sec mark this change in the character of the seismic section. On line 3, most of these reflectors stop at ~10.5 sec, and there are only scattered reflectors to 11 sec.

Within this laminated reflector zone (10 - 11 sec), there is a "splaying" of dip segments at 10.5 sec on line 1. (See Figure 6). Divergent and convergent dip segments are seen throughout the migrated lines, from 3 sec down. This character can not be seen as well on the unmigrated sections. In fact, in most places, one can not see it at all.

There is a high amplitude reflection ("bright spot") at 12.5 sec on line 2. (See Figure 2). It is easily seen on the unmigrated data, but it is without such marked amplitude contrast.

Interval velocities were calculated from the stacking velocities. Both are shown in Figure 7.

Figure 5. (next two pages) Portions of the unmigrated (left) and migrated (right) versions of line 2 (1-5 sec). Migrated at 5 km/sec to image ~ 2.5 -~4.5 sec. East is to the right. ~1:2 V.E.

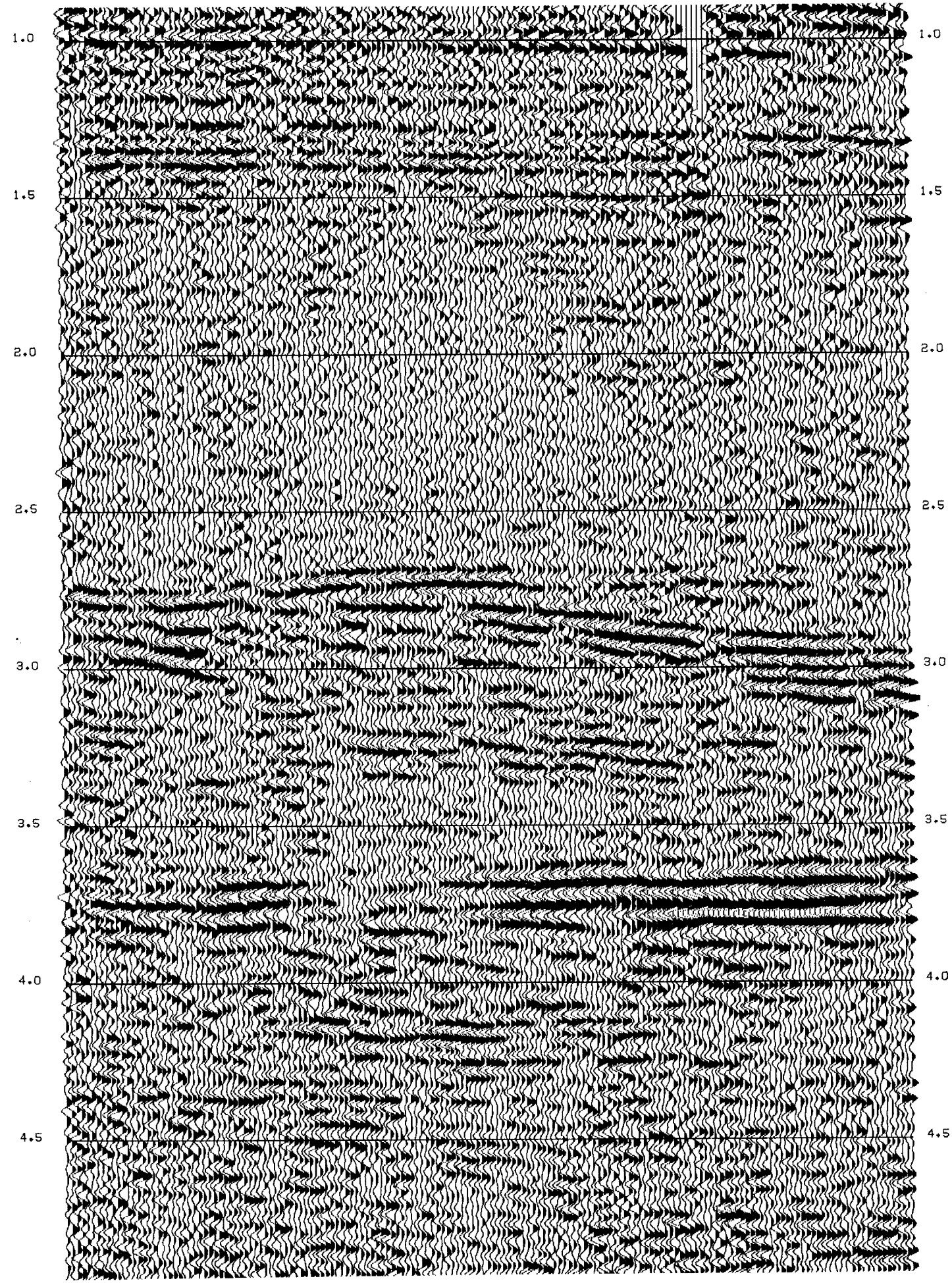
1.0
1.5
2.0
2.5
3.0
3.5
4.0
4.5
1.0
1.5
2.0
2.5
3.0
3.5
4.0
4.5

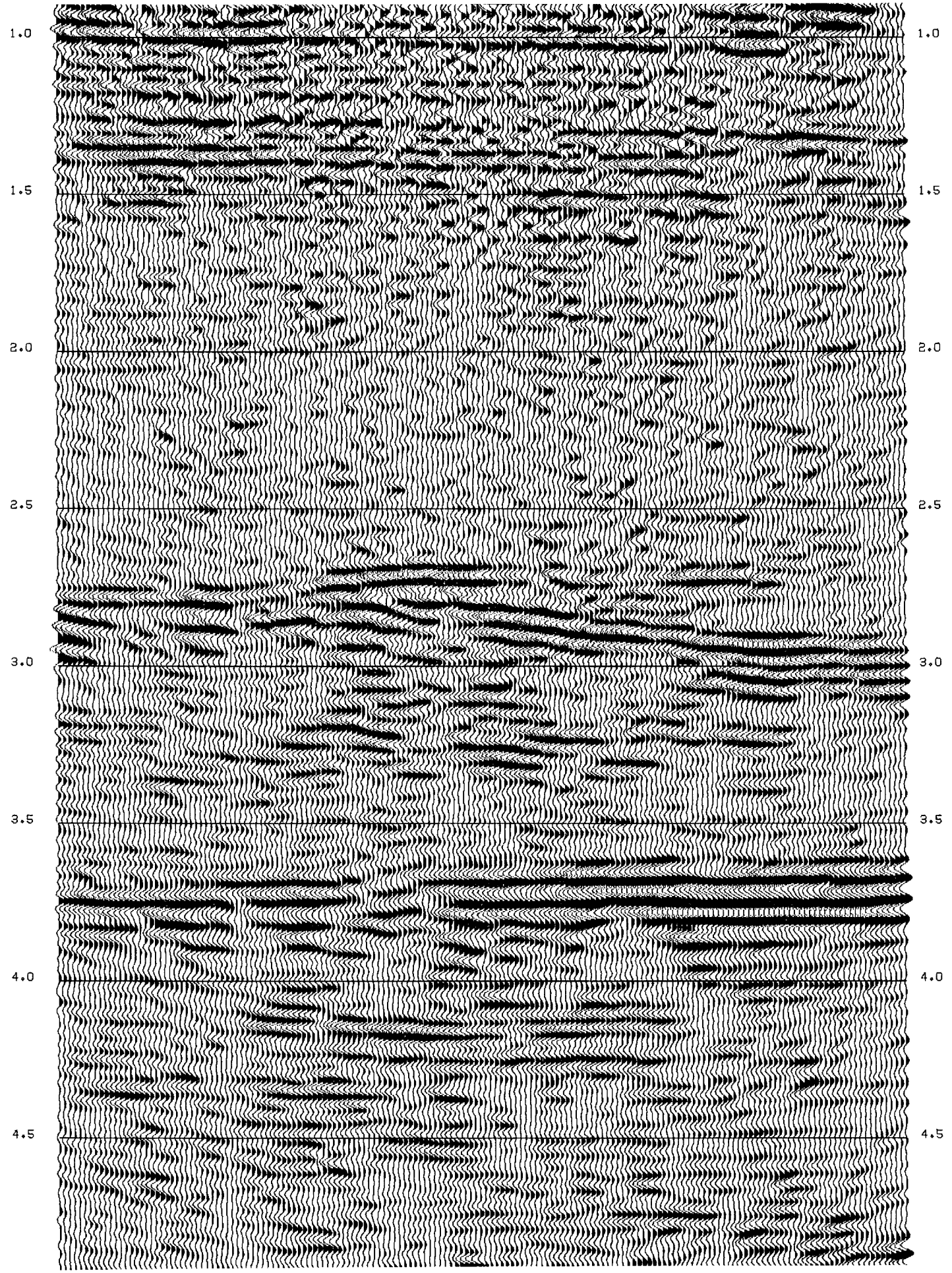
1.0
1.5
2.0
2.5
3.0
3.5
4.0
4.5

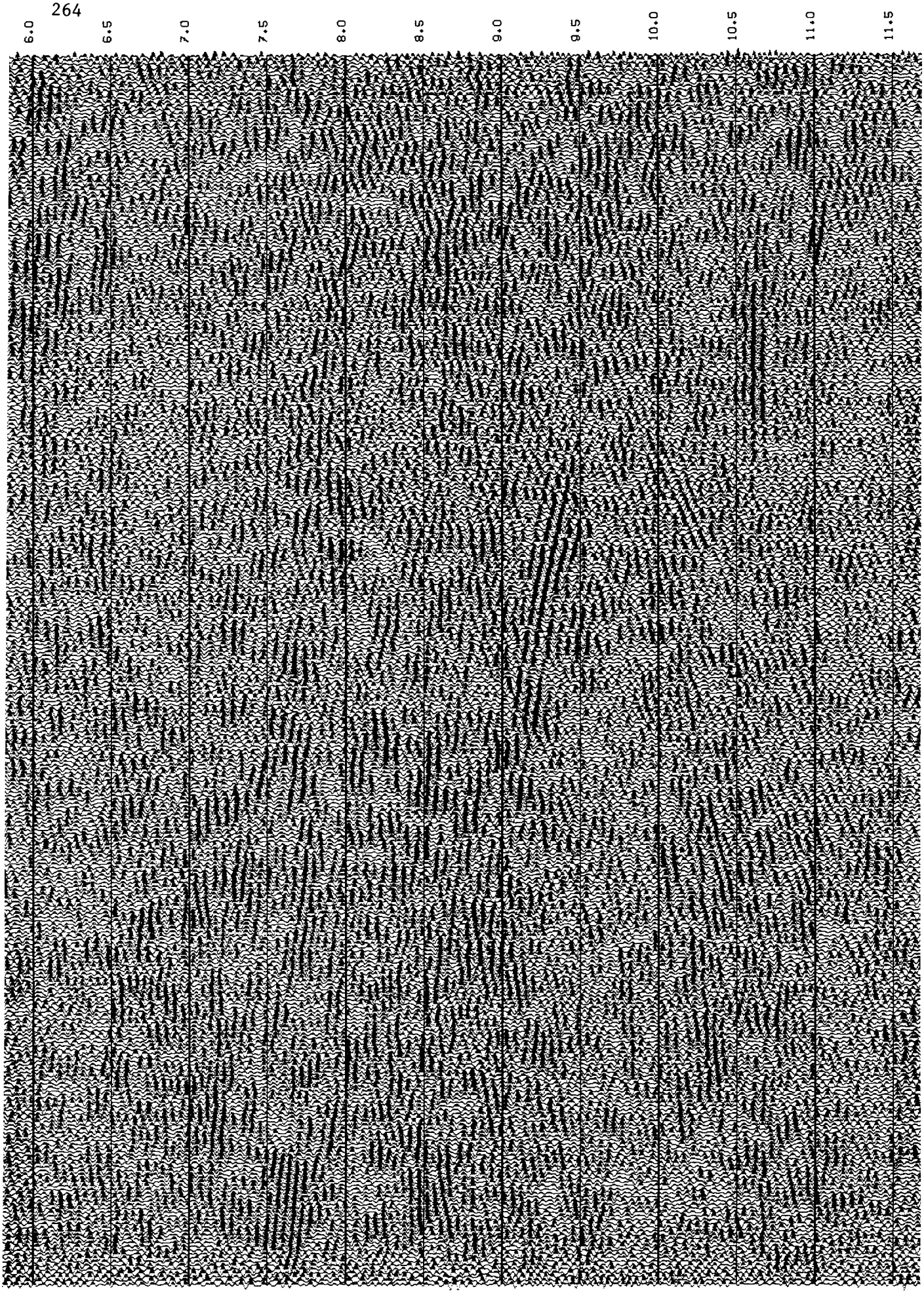

Figure 6. Portions of the unmigrated (left) and migrated (right) versions of line 1 (6-11.5 sec)

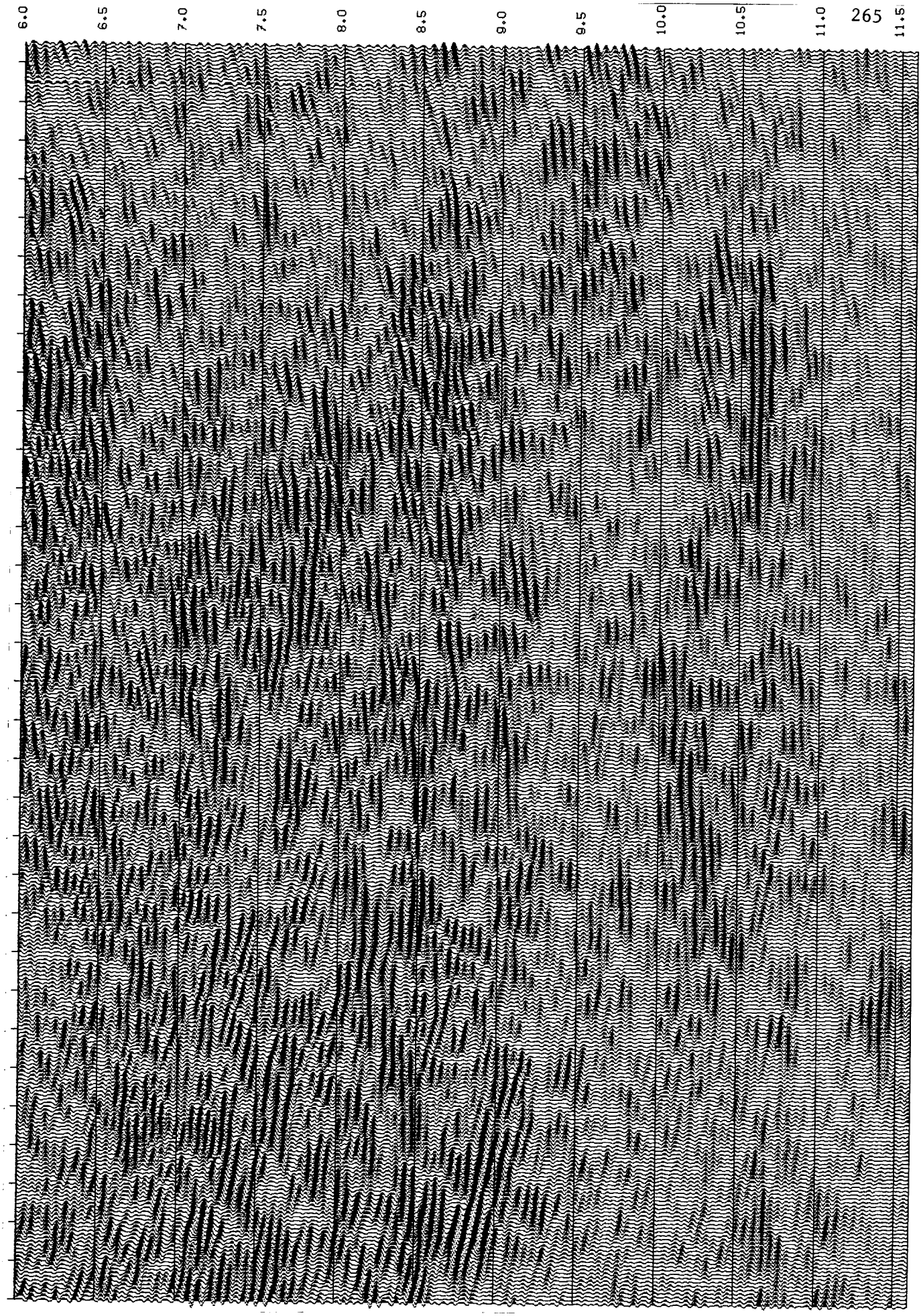

Migrated at 6 km/sec to image between 6 - 11 sec; south is to the right; scale is 1:1.

	Stacking Vel. (=RMS vel. if no dip) (m/sec)	Time (sec)	Interval Vel.
Velocity function 10	1830	0	3701
	3700	1.3	5715
	5160	2.76	5590
	5400	6.1	6447
	5920	11.6	7107
	6140	14.	(13,034) Not reliable
	6820	15.	
Velocity function 11	1830	0	3701
	3700	1.3	5838 ± 200
	4800	2.4	5495 ± 400
	5100	4.1	5968 ± 600
	5400	6.1	6447
	5920	11.6	7107
	6140	14.	(13,034) Not reliable
	6820	15.	
Velocity function 12	1830	0	3701
	3700	1.3	6856
	5640	2.85	7245
	6220	4.27	6671
	6500	11.02	7477
	6720	14.	(8041) Not reliable
	6820	15.	

Figure 7A. Stacking velocities for the Hardeman area; interval velocities calculated from Dix's equation,

$$v_i = \left(\frac{v_2^2 t_2 - v_1^2 t_1}{t_2 - t_1} \right)^{1/2}, \quad \text{assuming no dip.}$$

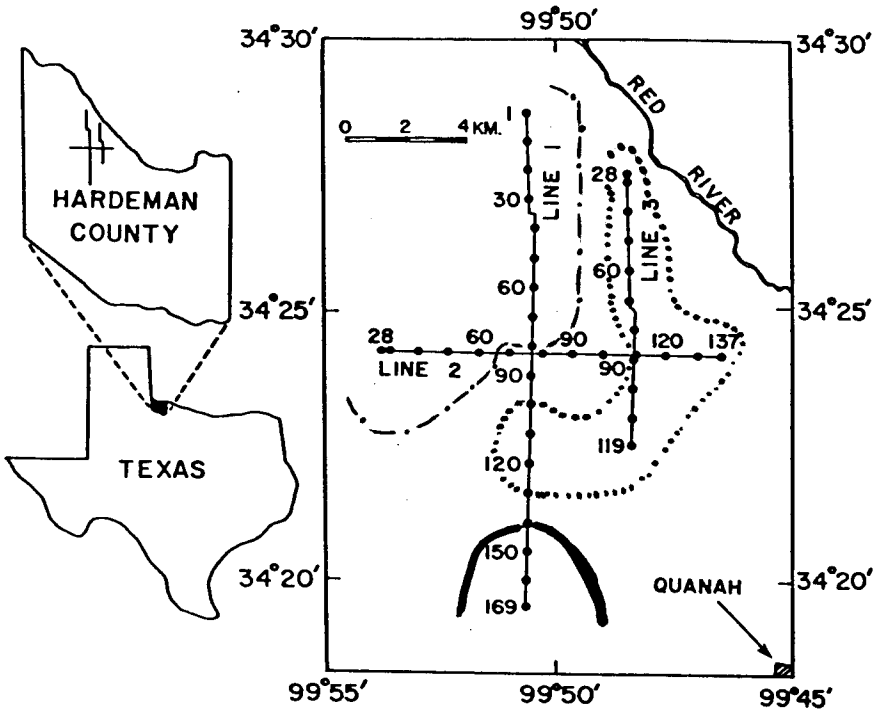

FIGURE 7B -- Extent of applicability of each velocity function. (-·-·- = velocity function 11; ——— = velocity function 12; • • • • • = velocity function 10.)

Unfortunately, detailed velocity scans were not available to Stanford at the time of this publication. A detailed velocity analysis is called for, but we are waiting on the re-gathering of the line by Petty-Ray.

Interpretation

The enhanced dipping-reflector continuity is one of the most striking effects of the migration, along with the collapsing of the large diffractions and spatial relocation of dipping events. We expect migrated lines to have a gradual increase in event continuity with time and a gradual decrease in amplitude with time, due to limited cable length and the shortness of the line. However, neither all the event continuity nor the abrupt decrease of amplitude at 11 sec can be explained simply by the migration of a line limited in extent.

The high amplitude event at 12.5 sec, line 2 (Figure 2), is not thought to be the Moho. While the amplitude of the reflector

indicates a marked velocity-density change at that interface, refraction work in southern Oklahoma (100 km to the NE) indicates that the Moho is ~50.9 km deep (Tryggrason and Qualls). The VIBROSEIS field records were recorrelated by Oliver and Kaufman using a shorter sweep to extend the record time from 15 sec to 18.5 sec. They concluded that the reflectors at 15.5 sec, about 50 km deep, probably mark the Moho.

Now we shall address the crux of the interpretation problem: the geologic explanation of the layered reflectors, the "dip segment splaying" observed, and the interval velocity information. To do this, the geologic setting of the Hardeman lines must be described. Then, the geologic horizons will be tentatively tied to the seismic reflections.

Basement geologists have abundant well information concerning basement in most of Texas. The authors describing basement (Muehlberger et al., 1967; Flawn, 1956) exhaustively analyzed hundreds of core samples, or used the analysis of such cores, for their articles. The oldest known basement rocks in Texas and eastern New Mexico are a 1570 - 1650 m.y. sequence of Precambrian gneiss, schist, and quartzite which is invaded extensively by granitic, granodioritic, and quartz-dioritic rocks. These rocks are labeled GN in Figure 8, a regional map showing the locations of the various basement rocks. Meta-sedimentary (schist, quartzite) and meta-igneous (metarhyolite, amphibolite) rocks (TOR, Figure 8) were metamorphosed 1350 m.y. ago, when some of the gneisses of GN were also further metamorphosed. The granites which intrude the metasedimentary sequence are 1300 - 1400 m.y. old. This region is thus interpreted as having a 1650 m.y. (or older) basement on which a cycle of sedimentation, metamorphism, and intrusion was superimposed (Muehlberger). (See Figure 9)

The Chaves granitic terrance (CH, Figure 8) is the next youngest basement rock (1350 m.y.) recognized in Texas. These rocks are largely granite, granodiorite, compositionally equivalent gneiss, and some metasediments and meta-igneous rocks. 80%

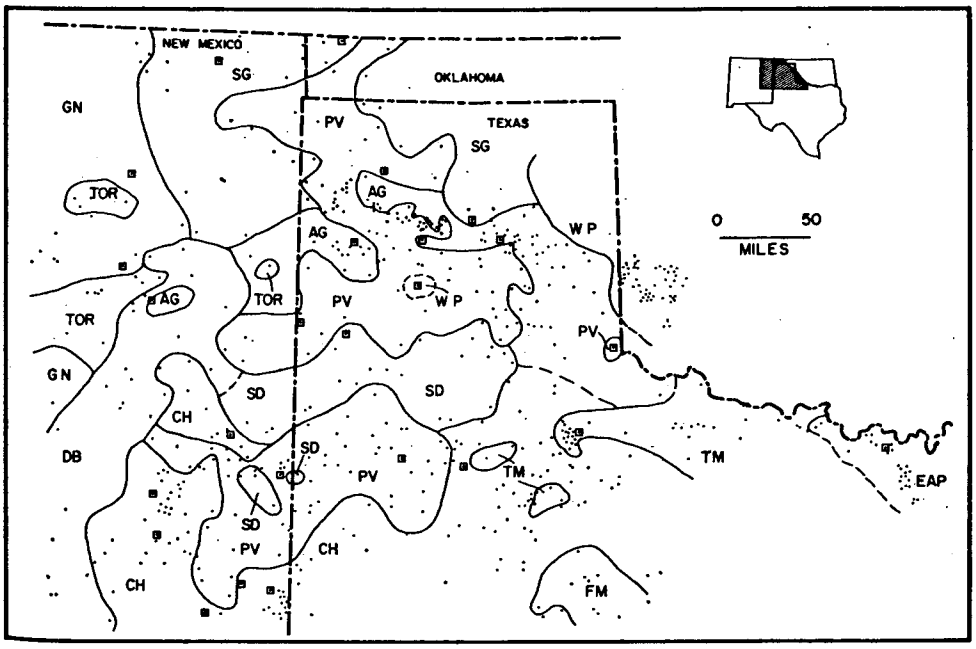

Geologic map of Precambrian rocks of Texas Panhandle and eastern New Mexico; includes Cambrian igneous rocks of Wichita province (WP). Dots = samples studied; squares = isotopic ages reported in Muehlberger *et al.* (1966); GN = older gneiss and granite; TOR = older metasedimentary and meta-igneous rocks; CH = Chaves granitic terrane; PV = Panhandle volcanic terrane; SD = Swisher diabasic terrane; AG = Amarillo granite terrane; SG = Sierra Grande granite terrane; DB = De Baca terrane; TM = Tillman metasedimentary group; FM = Fisher metasedimentary terrane; EAP = Eastern Arbuckle province. See text for discussion.

FIGURE 8 -- (from Muehlberger et al., 1967)

of the samples studied were granite in composition. Most of the metasedimentary rocks belonged to the green-schist facies, although well cores also sampled amphibolite and diorite gneiss. Figure 8 shows these rocks to be closer in space than the TOR metasediments.

The third terrane recognized as older basement in Texas is the Sierra Grande Granite terrane (SG, Figure 8). Dated at 1270 m.y., it is a medium - to coarse-grained biotite granite to granodiorite.

The Panhandle volcanic terrane (PV, Figure 8) overlies the above described units. It is an extensive supracrustal and shallow intrusive rhyolite porphyry - rhyolite tuff with smaller amounts of rhyodacite, trachyte, trachyandesite, and andesite. Several ignimbrite bodies are known by well cores. The extrusive

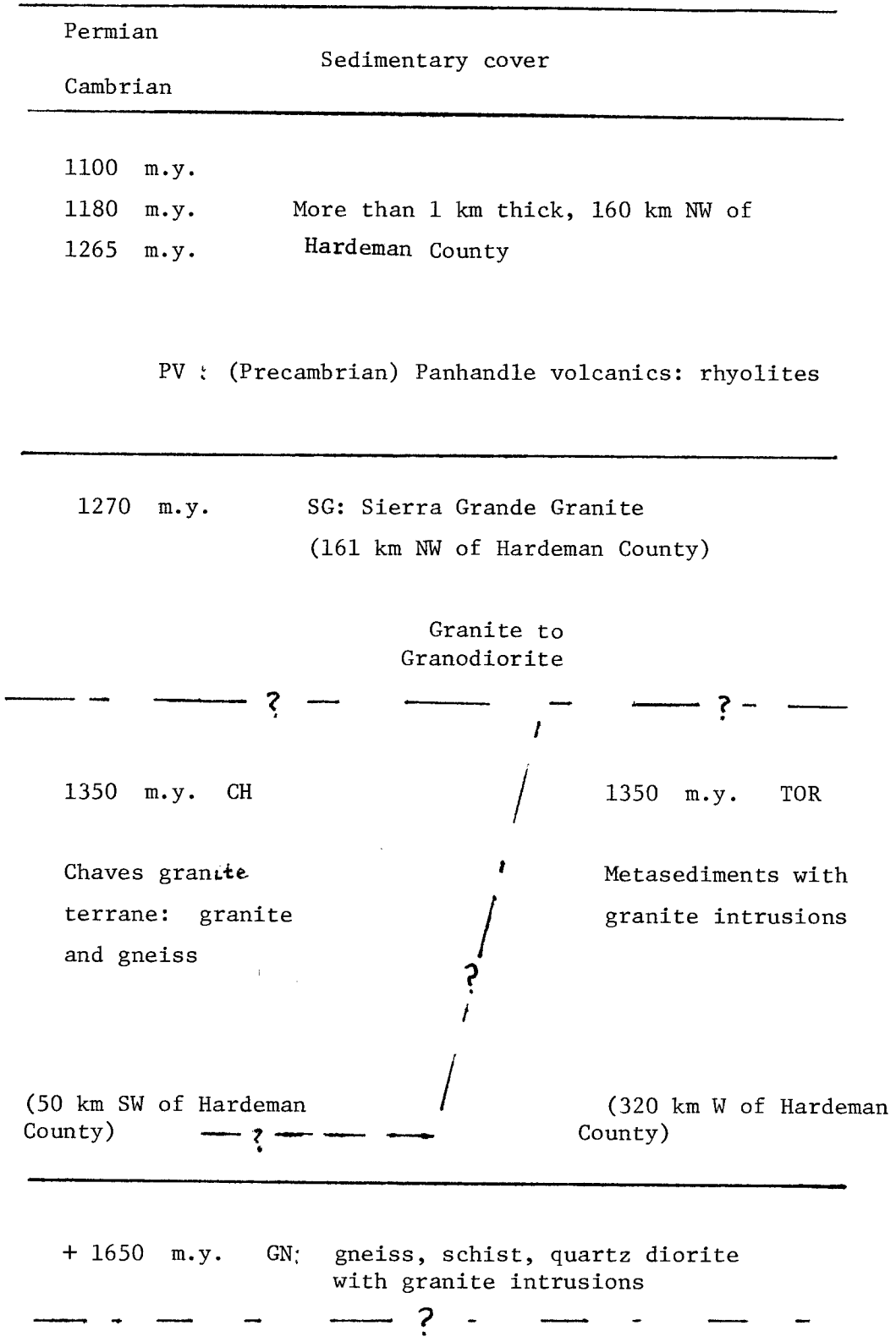

FIGURE 9 -- Generalized geologic column of Texas basement.

character of most of the rhyolites is established unequivocally by petrologic studies (Muehlberger et al.) These rhyolites are dated between 1100 and 1180 m.y. (Muehlberger et al., 1967). 1146 m of volcanic rock (with 79.3 m of diabase) was drilled without reaching basement in Potter County, 209 km to the NW of the Hardeman County lines. Cores from widely spaced wells showed only low dips on flowage structures, indicating that this thick, layered rhyolite is nearly horizontal (Muehlberger et al.). The 1265 ± 40 m.y. rhyolite drilled ~.5 km from the Hardeman lines may be within this Panhandle volcanic terrane, which thus extends the age of this sequence from 1100 to 1265 ± 40 m.y.

The Amarillo granite terrane (AG , Figure 8), shown as underlying most of Hardeman County, has an average age of 1140 m.y. (1100 -1190 m.y.), clearly younger than the 1265 m.y. sample from the well. Using Muehlberger's numbers, it is seen that this terrane is closely associated in time with the Panhandle volcanics. This granite terrane is comprised of one and two feldspar granites and granodiorites, with considerably less silicic granites found in the eastern Panhandle (near Hardeman) than in the western extent of this terrane. In the central Panhandle, granite intruded rhyolite, and in northeast Potter County (241 km to the NW), a granite sill above metarhyolite was drilled. The AG terrane is probably not present under the Hardeman lines, because basement there is the older PV rhyolite.

We will now tie together the stratigraphic information with the seismic section. From 0 to 1.6 sec, we are in Permian to Cambrian sedimentary section. At 1.6 sec Precambrian 1265 m.y. rhyolite (Panhandle volcanics) starts. This rhyolite (compositionally equivalent to granite) probably overlies the SG terrane and thus we see granite grading to granodiorite down to 2.8 sec. Scattered faint reflectors (Figure 2) perhaps show the gradation from a rhyolite to a fast (+6.0 km/sec) velocity granodiorite at 2.8 sec. The strong reflector at 2.8 sec could be the start of the CH granite terrane in the form of the top of a (slower velocity) silicic granite sill, or cluster of sills. The base of the

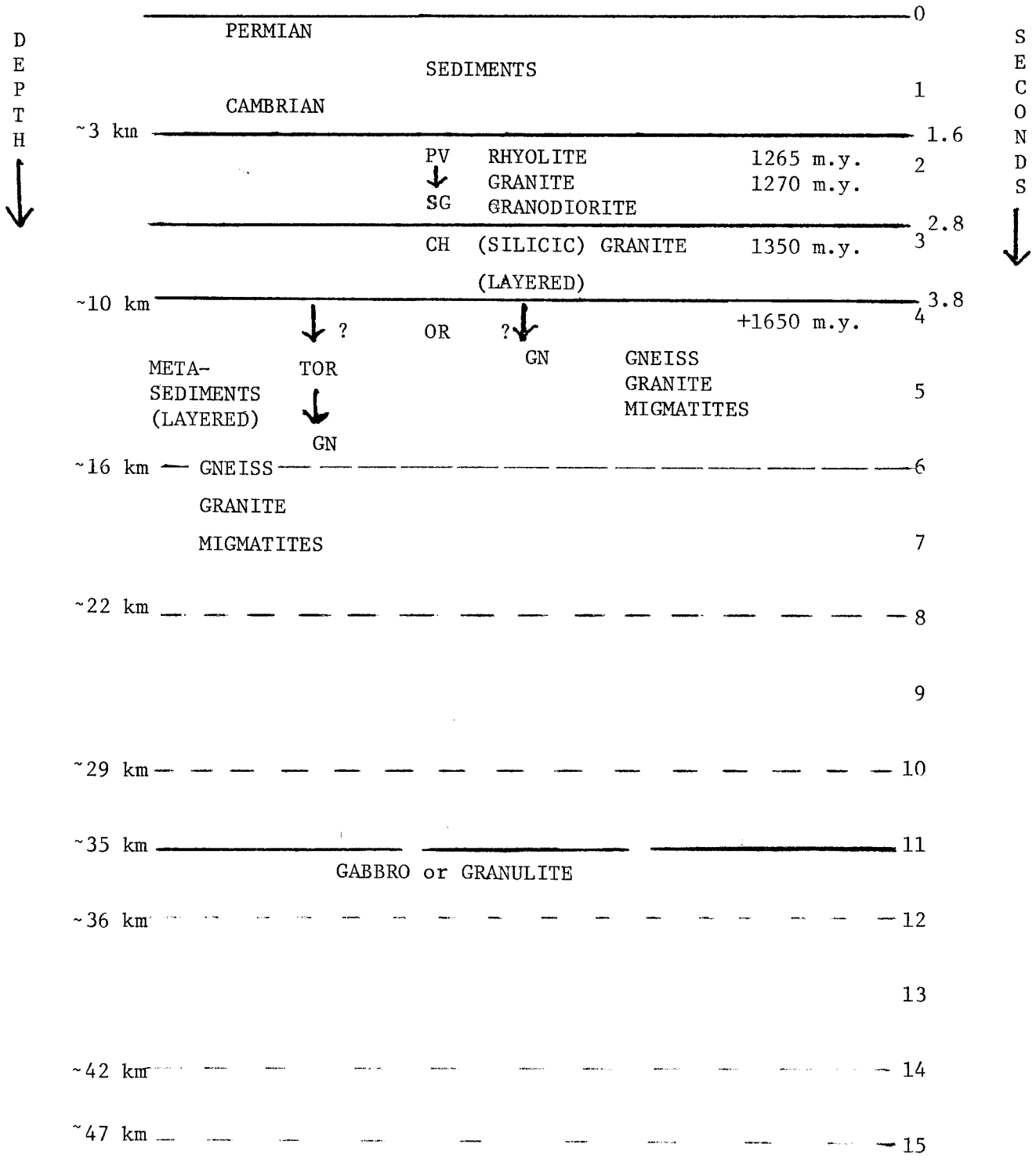

FIGURE 10: Tentative theory of seismic lines to basement geology.

CH granite could be the strong reflector 3.8 sec, whereupon we enter either TOR-type metasediments underlain by GN-type gneisses, or we enter GN type gneiss and quartz diorite directly. At this depth (~10 km) we may be looking at migmatites (alternating layers or lenses of granite types and schists or gneisses). Mueller (1977) postulates these rocks to be the European middle crustal layer (13-21 km depth). This interpretation is shown schematically in Figure 10. The different "levels" of reflector density may be gradationally higher metamorphic zones or "fronts". The convergent and divergent dips segments seen, i.e., the splaying of dip segments, could be energy from out of the plane of section. However, it is hard to believe that all of the convergent/divergent dip segments are from out of the plane. Zones of low reflector density may be regions of granite intrusions, as between 9 - 10 sec on line 1 (see Figure 4). Oliver et al. postulated zones of low reflector density to be plutons in his interpretation of the unmigrated data, but the spatial location of his postulated intrusions is shown to be invalid upon inspection of the migrated data.

At 11 sec, where the seismic character of the section changes, and the interval velocities probably change from 6.4 (± .5 km/sec) to 7.2 (± .5 m/sec), we may be seeing the change from granites and gneisses to gabbro, granulite, and/or amphibolite. The strong reflector at 12.5 may be a "hard streak" (peridotite? eclogite?) within the gabbro or granulite.

Since the longest Hardeman line is only 16.6 km long, all strict interpretation should be addressed to the section above 8 km (3.5 sec). However, it seems foolish not to offer tentative interpretations of the entire section.

While the interval velocities cited in Figure 5 have significant error bars, and while the error bars become even greater at depth, the above geologic interpretation is not contradicted by existing data. Crustal inhomogeneity is especially suggested within these lines, wherein the interval between 3 and 4 sec is usually lower in interval velocity than adjacent formations, but

on the south end of line 1, is higher in velocity than the adjacent formations. In this paper we did not use velocity function 12 (the fast one); velocity scans to verify this higher velocity function are needed. The interval velocity estimates from the seismic RMS velocities agree fairly well with the refraction velocities measured by Tryggvason and Qualls (1967) and Mitchell and Landisman (1970). Their results are shown in Figures 11 and 12.

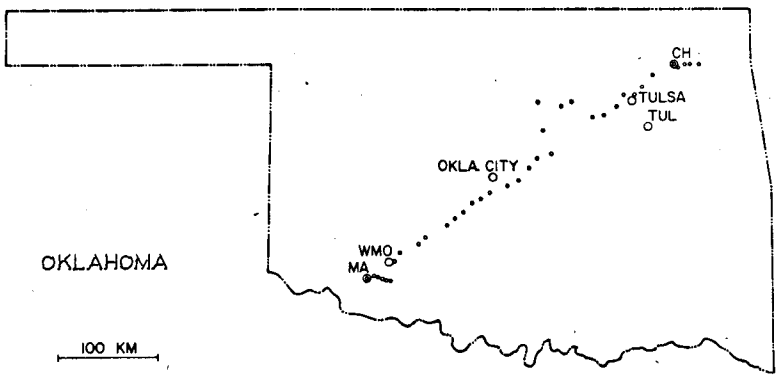

Location of the refraction profile in Oklahoma 1964. The two permanent seismological observatories in Oklahoma, Wichita Mountains Observatory (WMO) and Leonard Observatory (TUL) are shown. Shot points, double circles; recording sites, small circles.

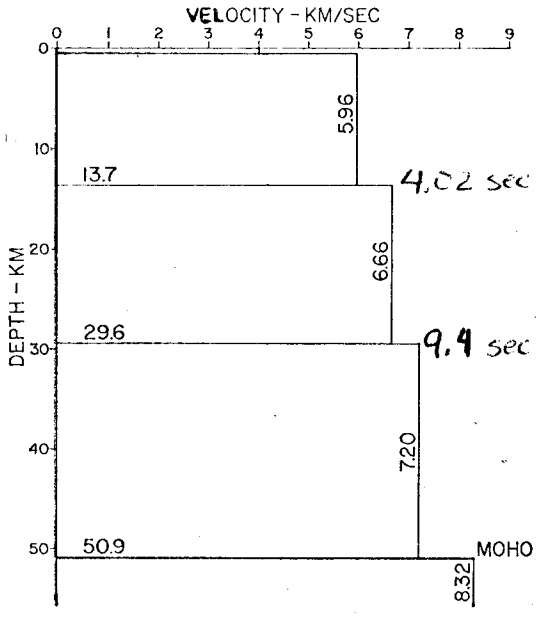

Oklahoma earth model assuming homogeneous horizontal layers.

FIGURE 11 -- Results of Tryggvason & Qualls (1967) seismic refraction work in southern Oklahoma.

FIGURE 12. Results of Mitchell and Landisman's (1970) refraction work in southern Oklahoma, 100 km NE of Hardeman County, Texas.

VELOCITY–DEPTH VALUES

Manitou division		Chelsea division	
Depth (km)*	Compressional velocity (km/sec)	Depth (km)*	Compressional velocity (km/sec)
		0	4.00
		0.6	4.00
		0.6	6.05
		1.0	6.05
−0.2	5.50	1.0	5.50
0.8	5.50	3.1	5.50
0.8	6.04	3.1	6.04
3.8	6.12	6.1	6.12
10.3	6.05	13.4	6.04
10.3	6.48	13.4	6.48
15.4	6.50	16.4	6.50
15.4	6.20	16.4	6.20
17.9	6.20	17.9	6.20
17.9	6.68	17.9	6.68
26.1	6.75	26.1	6.75
26.1	7.01	26.1	7.01
35.2	7.09	35.2	7.09
35.2	7.33	35.2	7.33
46.3	7.39	46.3	7.39
46.3	8.17	46.3	8.17

* Depth is measured from a datum level of 0.4 km above sea level.

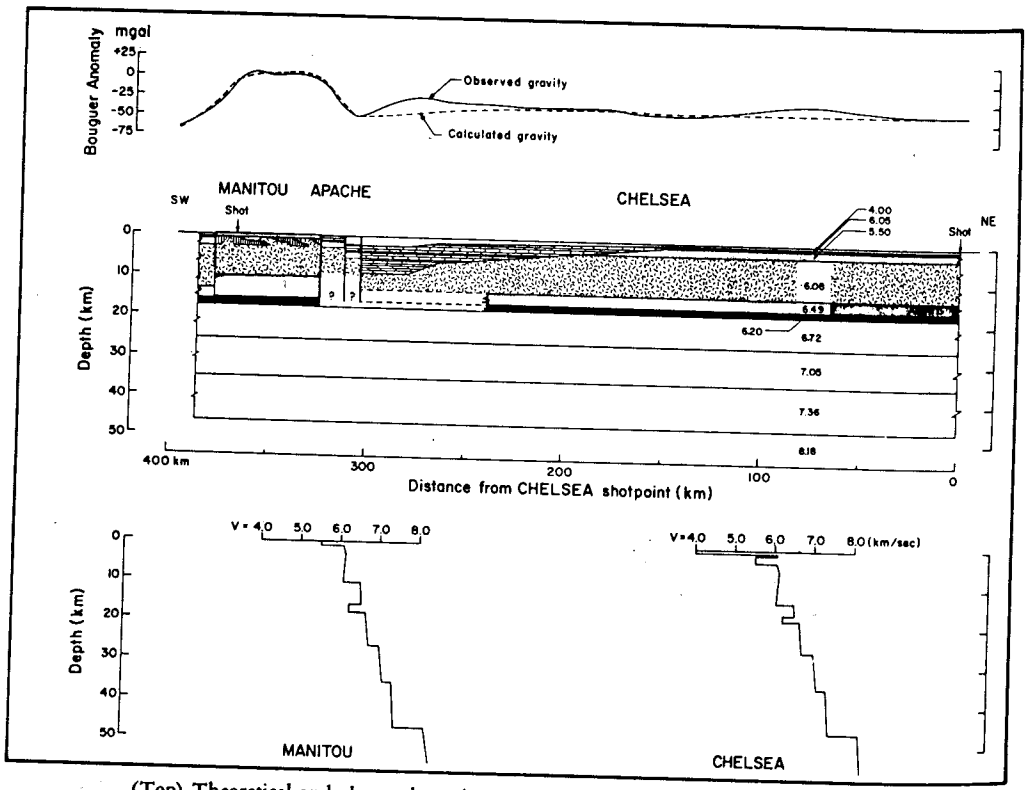

(Top) Theoretical and observed gravity anomaly values along the profile. (Middle) Crustal model with average velocity values indicated for each layer. Dotted lines indicate uncertain positions of boundaries. The limestone symbol only implies fast sediments and does not necessarily indicate limestone or flat-lying beds. Vertical exaggeration: X2. (Bottom) Velocity-depth curves near the Chelsea and Manitou shot points.

We hope to refine this "first-pass" estimate of seismic reflection velocities with the results of a detailed velocity analysis.

Birch's (1960) tables of compressional wave velocity in rocks up to 10 kilobars were used as the source of rock velocities to compare with seismically derived velocities. Figure 13 (based on Birch's work and others, taken from Bateman and Eaton, 1967) shows rock types of interest, with their velocities and densities.

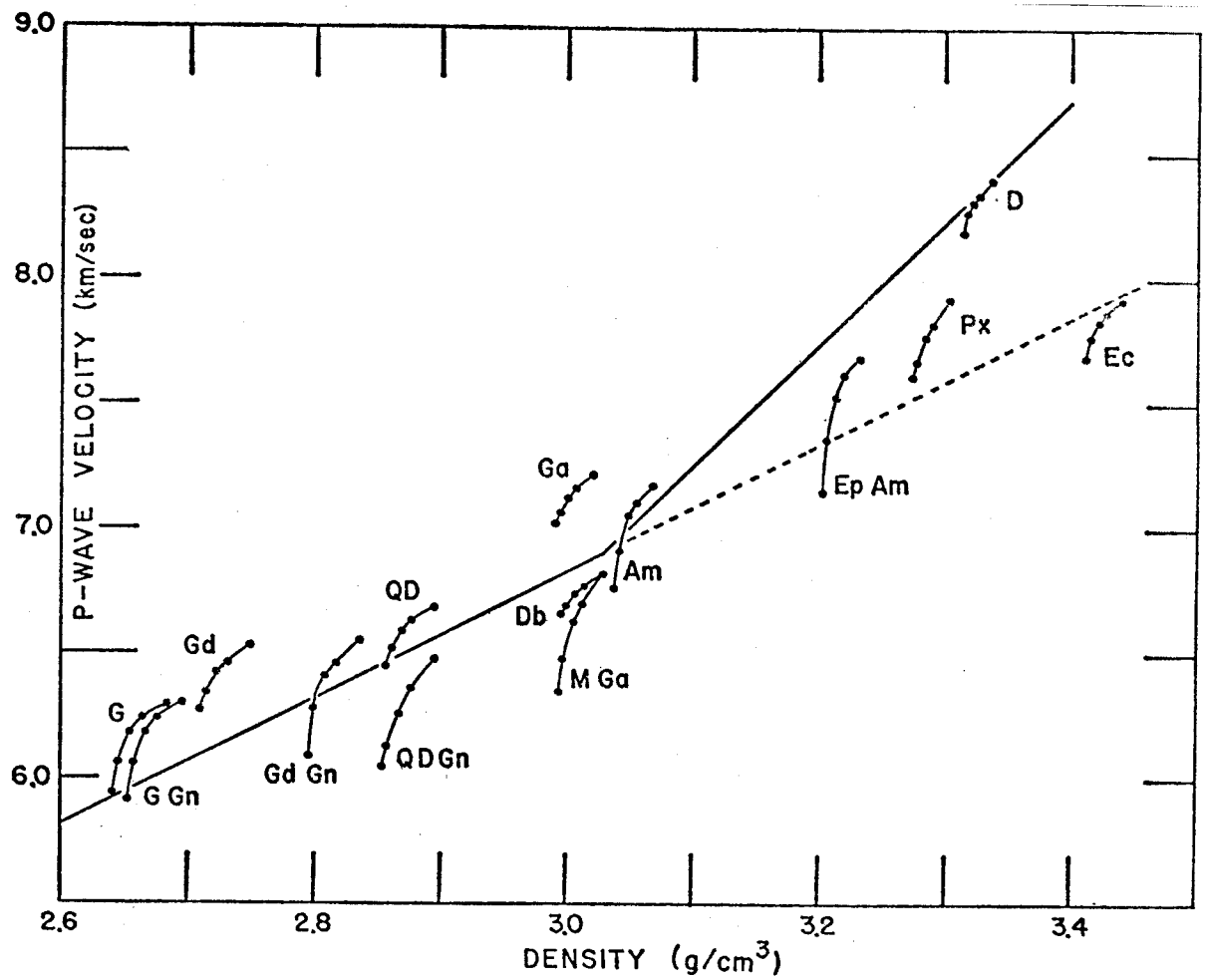

Experimental data (*15, 16*) on P-wave velocities as a function of confining pressure for selected igneous and metamorphic rocks. From bottom to top, data points for each rock type correspond to pressures of 1, 2, 4, 6, and 10 kilobars. The solid curve based on these data was used to estimate densities of the rocks composing the seismic columns from their velocities. Approximate lithostatic pressures corresponding to the tops of the seismic "layers" are plotted opposite the appropriate layer velocities at left. *G*, Granite from (i) Westerly, Rhode Island, (ii) Chelmsford, Massachusetts, and (iii) Barre, Vermont, and quartz monzonite from Porterville, California (*15*); *GGn*, gneiss 1 and gneiss 2 (*16*) from Berkshire Highlands; *Gd*, granodiorite from Butte, Montana (*15*); *GdGn*, gneiss 3 and gneiss 4 (*16*) from Berkshire Highlands; *QD*, quartz diorite from San Luis Rey, California, and Dedham, Massachusetts (*15*); *QDGn*, gneiss 5 from Berkshire Highlands (*16*); *Ga*, gabbro from Mellon, Wisconsin, and French Creek, Pennsylvania, and norite from Pretoria (*15*); *Db*, diabase from (i) Holyoke, Massachusetts, (ii) Centerville, Virginia, (iii) Sudbury, Ontario, and (iv) Frederick, Maryland (*15*); *MGa*, metagabbro from Hodges Mafic Complex (*16*); *Am*, amphibolite 1 and amphibolite 2 (*16*) from Mount Tom; *EpAm*, epidote amphibolite 1 and epidote amphibolite 2 (*16*) from Hodges Mafic Complex; *Px*, pyroxenite from Sonoma County, California, and bronzitite from Stillwater Complex and Bushveld Complex (*15*); *D*, dunite from Twin Sisters Peaks, Washington (*15*); *Ec*, eclogite from Healdsburg, California, and Kimberly (*15*).

Figure 13. Rock velocities and densities (-from Bateman and Eaton, 1967).

Conclusions

Migration yielded sections wherein substantial additional knowledge about the crust in Hardeman County was gained, even though the amount of dipping information recorded was limited due to the shortness of the lines (11 - 16.6 km). This suggests strongly that the migration of the Wyoming COCORP line(s) will yield even more knowledge, since 52.5 km is currently available and shortly an additional 116 km will be released.

The migration of the Hardeman deep crustal seismic reflection lines more clearly imaged the crust. Layering is delineated within the intermediate crust, and zones of "no reflectors" are seen in their correct spatial location. The upper and intermediate crust, the "transparent" zone between 9 - 10 sec (on line 1), the laminated reflectors between 10 and 11 sec, and the nature of the discontinuity at 11 sec become more obvious.

Appendix

Field Procedure

Petty-Ray Geophysical, Inc., of Houston, Texas, was engaged for the data acquisition and computations. The field acquisition unit was a 48-channel MDS 8/Mandrel Data System; geophones were Electro-Technical Laboratory EV22C with a natural frequency of 7½ Hertz; the VIBROSEIS technique was used, sources being five synchronized vibrators (three Y1100, each of 13½ ton peak force, and two Y900, each of 10½ ton peak force).

Two days were spent prior to production work to establish the field parameters. Studies of source-generated surface and near-surface waves were made using single location sources and podded geophone spreads. Various arrays of vibrators and vibrator signal frequencies were studied. The parameters chosen for the production work were the following:

In-line source and geophone arrays.

Station spacing: 100 m (330 ft), geophone spread length 4.7 km (15,510 ft).

Distance of source station to nearest geophone: 400 m (1,320 ft).

24 geophones per station, spread over a distance of 200 m (660 ft) (100 percent geophone overlap).

Vibrator array: (Y900 — Y1100 — Y1100 — Y1100 — Y900) vibrators 18.3 m (60 ft) apart, move-up interval of 6.5 m (20 ft); 16 sweeps summed per record.

Pilot signal: 15 sec duration; upsweep, 10 to 32 Hertz.

8 msec sampling interval; 30 sec recording duration.

Normal vibrator locations were spaced two stations apart.

The Hardeman County experiment was designed to provide data for twelvefold **CDP** stacking, and automatic gain control (AGC) was applied to keep amplitudes relatively uniform as a function of time. This processing was applied to the data to produce the sections shown in Figures 2A, 2B, and 2C. Other forms of processing have been applied to the data, or portions of it, but the results are not presented here.

- from Oliver et al., 1976.

References

Bateman, P.C., and J.P. Eaton (1967), Sierra Nevada Batholith, *Science*, 158, 1407-1417.

Birch, F. (1960), The velocity of compressional waves in rocks to 10 kilobars, *JGR*, 65, 1083-1102.

Flawn, P.T. (1956), *Basement Rocks of Texas and Southeast New Mexico*, Texas Univ. Bur. Econ. Geol. Publ., no. 5605, 261 p.

Mitchell, B.J. and M. Landisman (1970), Interpretation of a crustal section across Oklahoma, *GSA Bull.*, 81, 2647-2656.

Muehlberger, W.R., R.E. Denison, and E.G. Lidiak (1967) Basement rocks in continental interior of United States, *Am. Assoc. Petr. Geol. Bull.*, 51, 2351-2380.

Mueller, Stephan (1977), A new model of the continental crust, *AGU Monograph* 20, 289-317.

Oliver, J., M. Dobrin, S. Kaufman, R. Meyer, and R. Phinney (1976) Continuous seismic reflection profiling of the deep basement, Hardeman County, Texas, *Geol. Soc. Amer. Bull.*, 87, 1537-1546.

Oliver, J., S. Kaufman (1977) Complexities of the deep basement from seismic reflection profiling, *AGU Monograph* 20, 243-253.

Stolt, R. (1978) Migration by Fourier transform, *Geophysics*, 43, 23-48.

Tryggvason, E. and B.R. Qualls (1967) Seismic refraction measurements of crustal structure in Oklahoma, *JGR* 72, 3738-3740.